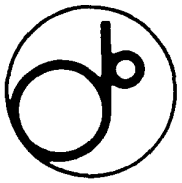

KEK Preprint 93-97
AMY 93-2
August 1993
H

Measurements of inclusive jet production in almost-real $\gamma\gamma$ collisions at TRISTAN

The AMY Collaboration

Submitted to the XVI International Symposium on Lepton and Photon Interactions, Cornell University, Ithaca, New York, August 10 - 15, 1993.

National Laboratory for High Energy Physics, 1993

KEK Reports are available from:

Technical Information & Library
National Laboratory for High Energy Physics
1-1 Oho, Tsukuba-shi
Ibaraki-ken, 305
JAPAN

Phone: 0298-64-1171
Telex: 3652-534 (Domestic)
(0)3652-534 (International)
Fax: 0298-64-4604
Cable: KEK OHO
E-mail: LIBRARY@JPNKEKVX (Bitnet Address)
library@kekvax.kek.jp (Internet Address)

Measurements of inclusive jet production in almost-real $\gamma\gamma$ collisions at TRISTAN

The AMY Collaboration

ABSTRACT

We present cross section measurements for inclusive jet production in almost-real $\gamma\gamma$ collisions at TRISTAN using AMY detector. The results are compared with leading-order QCD calculations for different parameterizations of the parton density in the photon.

Submitted to the XVI International Symposium on Lepton and Photon Interactions, Cornell University, Ithaca, New York, August 10-15 1993.

Measurements of inclusive jet production in almost-real $\gamma\gamma$ collisions at TRISTAN

The AMY Collaboration

B.J.Kim [a], T.Nozaki [b], A. Bodek [a], T.Kumita [a], Y.K. Li [a], C.Velisarris [a], R.Walker [a], K.Abe [b], R.E.Breedon [b,h], Y.Fujii [b], Y.Kurihara [b], F.Liu [b], A.Maki [b], T.Omori [b], H.Sagawa [b], Y.Sakai[b], T.Sasaki [b], Y.Sugimoto [b], Y.Takaiwa [b], S.Terada [b], P.Kirk [c], C.P.Cheng [d], W.X.Gao [d], W.G.Yan [d], M.H.Ye [d], A.Abashian [e], K.Gotow [e], D.Haim [e], M.E.Mattson [e], N.Morgan [e], L.Piilonen[e], K.L.Sterner [e], S.Lusin [f], C.Rosenfeld [f], S.Wilson [f], L.Y.Zheng [f], C.A.Fry [g], R.Tanaka [g], L.M.Chinitz [h], Winston Ko [h], R.L.Lander [h], J.Rowe [i], J.R.Smith [h], D.Stuart [h], S.Kanda [i], S.L.Olsen [i], K.Ueno [i], F.Kajino [j], R.Poling [k], T.Thomas[k], T.Aso [l], K.Miyano [l], H.Miyata [l], M.Oyoshi [l], Y.Yamashita [m], M.H.Lee [n], F.Sannes [n], S.Schnetzer [n], R.Stone [n], J.Vinson [n], S.Kobayashi [o], A.Murakami [o], S.K.Sahu [o], M.E.Zomorrodian [o], K.B.Lee [p], Y.S.Chung [p], J.S.Kang [p], K.W.Park [p], S.K.Kim [q], S.S.Myung [q], S.K.Choi [r], D.Son [r], S.Ebara [s], S.Matsumoto [s], N.Takashimizu [s], and T.Ishizuka [t]

[a] *University of Rochester, Rochester, NY 14627, USA*
[b] *KEK, National Laboratory for High Energy Physics, Ibaraki 305, Japan*
[c] *Louisiana State University, Baton Rouge, LA 70803, USA*
[d] *Institute of High Energy Physics, Beijing 100039, China*
[e] *Virginia Polytechnic Institute and State University, Blacksburg, VA 24061, USA*
[f] *University of South Carolina, Columbia, SC 29208, USA*
[g] *SSC Laboratory, Dallas, TX 75237, USA*
[h] *University of California, Davis, CA 95616, USA*
[i] *University of Hawaii, Honolulu, HI 96822, USA*
[j] *Konan University, Kobe 658, Japan*
[k] *University of Minnesota, Minneapolis, MN 55455, USA*
[l] *Niigata University, Niigata 950-21, Japan*
[m] *Nihon Dental College, Niigata 951, Japan*
[n] *Rutgers University, Piscataway, NJ 08854, USA*
[o] *Saga University, Saga 840, Japan*
[p] *Korea University, Seoul 136-701, South Korea*
[q] *Seoul National University, Seoul 151-742, South Korea*
[r] *Kyungpook National University, Taegu 702-701, South Korea*
[s] *Chuo University, Tokyo 112, Japan*
[t] *Saitama University, Urawa 338, Japan*

1. Introduction

Resolved photon processes in $\gamma\gamma$ collisions are hard, non-diffractive hadronic interactions where a constituent parton in one of the photons interacts with the other photon or one of its constituents. In these processes, the interacting constituents produce wide-angle jets and the noninteracting constituents produce spectator jets in the directions of the incident photons. Hadron-jet production via resolved photon processes in high energy real $\gamma\gamma$ collisions was first discussed in 1978-1979 by Brodsky *et al.*,[1] and Kajantie and Raito.[2] The possibility of using measurements of resolved photon processes at existing accelerators to determine the parton densities in the photon was pointed out recently by Drees and Godbole.[3]

While data from PEP and PETRA experiments show some indications of resolved photon processes,[4,5] the first clear experimental evidence for them was reported by the AMY group at TRISTAN.[6] Subsequently, the H1 and ZEUS experiments reported observations of resolved photon processes in γp collisions at the HERA ep collider.[7,8] Recently the TOPAZ group at TRISTAN has also observed resolved photon processes.[9] Resolved photon processes are expected to be the dominant source of high-p_t hadron production in very high energy e^+e^- collisions and have been identified as a potentially serious background for experiments at future linear colliders.[10] Precise measurements of resolved photon processes at existing energies will help provide realistic estimates of these background levels.

We report on an experimental study of jet production in high energy $\gamma\gamma$ collisions. The experiment uses reactions of the type $e^+e^- \rightarrow e^+e^- + hadrons$ at $E_{cm} \simeq 60\ GeV$, where both the electron and positron scatter at small angles (untagged events) and the virtual photons are nearly on the mass shell.

The experimental results reported here are based on a 27.2 pb^{-1} data sample accumulated in the upgraded AMY detector (AMY-1.5) at the TRISTAN e^+e^-storage ring. Results based on a 27.5 pb^{-1} data sample taken in the original AMY detector

(AMY-1.0) have already been published.[6] The AMY-1.5 detector has improved coverage in the forward-backward angular regions. In addition, the current analysis uses a Monte Carlo calculation of the resolved photon processes (MJET) that has been improved to include the effects of:

- the finite mass of the charm quark;
- the finite intrinsic p_t of the spectator jet; and
- string fragmentation[11] of quarks and partons.*

In ref. 6, we reported the results of a thrust analysis in the center of mass system of the detected hadrons where hadrons from the spectator jets were included. The events were divided into two hemispheres defined by the plane perpendicular to the thrust axis, the particles in each hemisphere combined into jets, and the component of the jet momentum relative to the beam direction denoted as P_T^{jet}. The observed thrust and P_T^{jet} distributions clearly indicate that contributions from resolved photon processes are needed to reproduce the data. In the present analysis we study jets produced by hard scattering processes and evaluate inclusive jet cross sections in almost-real $\gamma\gamma$ collisions. The similar analysis was done by the TOPAZ group.[9] There are two advantages of the present analysis over the previous one: the results do not suffer from any ambiguity in the simulation of the spectator jets, such as the unknown value of the intrinsic p_t of the spectator jet; and the jet cross sections have a clear correspondence to parton-level cross sections, which can be directly compared to theory.

2. Event selection

In the 1989 upgrade, the two different endcap shower counters (PTC, RSC) of AMY-1.0 were replaced by the single shower counter (ESC) of AMY-1.5. This upgrade provided a more uniform coverage for photons and electrons and extended the angular

*In our previous paper[6] we stated that the string fragmentation scheme was used. We recently found that the calculations reported in this paper used, in fact, the independent fragmentation scheme.

acceptance to $\theta \geq 13^0$. In this analysis we use only the data taken in 1990, which corresponds to a portion of the AMY 1.5 data. The details of the AMY detector has been reported elsewhere.[13]

Untagged hadronic events produced by $\gamma\gamma$ interactions are selected by requiring:

- a minimum of four charged tracks with polar angles in the range $25° \leq \theta \leq 155°$; of these at least two must have $|p| > 0.75$ GeV/c and at least one must have $p_t > 1.0$ GeV/c;
- the most energetic cluster appearing in the calorimeter, covering $|\ cos\theta\ | \leq 0.97$, must have an energy less than $0.25E_{beam}$ (anti-tagging);
- the net charge of the observed charged tracks $\sum q_i \leq 2$;
- the net transverse momentum limited to $|\sum \vec{p}_{t,i}| \leq 5.0\ GeV/c$, where $\vec{p}_{t,i}$ are the projections of the observed momenta on the plane transverse to the beam; and
- the invariant mass of observed hadrons must be in the range 4 GeV/$c^2 \leq W_{vis} \leq$ 20 GeV/c^2, where the calculation of W_{vis} includes both charged and neutral particles and assigns a pion mass to all charged particles.

The 3248 events that survive these cuts were visually scanned by physicists. In the scan, 451 events were attributed to stray beam particles interacting in the wall of the vacuum chamber and were discarded.

Hadronic annihilation events with either initial state radiation or a large amount of missing energy can satisfy the $e^+e^- \rightarrow e^+e^- + hadrons$ selection criteria. The level of this contamination was estimated using an event sample generated by the Lund 6.3 event generator[12] and passed through a detector simulation program. The contamination from $e^+e^- \rightarrow \tau^+\tau^-$ and $e^+e^- \rightarrow e^+e^-\tau^+\tau^-$ was also estimated by using Monte Carlo simulated events for these processes. We obtained the following background estimates:

- hadronic annihilation: 73 $\pm$ 6 events;

- $e^+e^- \rightarrow e^+e^-\tau^+\tau^-$: 66 $\pm$ 6 events; and
- $e^+e^- \rightarrow \tau^+\tau^-$: negligibly small.

From the distribution of vertex positions along the beam line we conclude that the residual contamination from beam-gas events is negligibly small.

The trigger efficiency for $e^+e^- \rightarrow e^+e^- + hadrons$ events that satisfy the selection criteria was estimated using a Monte Carlo simulation to be $97.1 \pm 1.8\%$. After all background subtractions and efficiency corrections, we obtain a final count of 2738 ± 76 events. The stated error is the quadrature sum of the statistical errors (1.9%) and the systematic uncertainties in the luminosity measurements (1.8%), trigger efficiency (1.6%), and scanning efficiency (2%).

3. Monte Carlo simulations

The experimental data are compared with the predictions of models for jet production in $\gamma\gamma$ reactions using Monte Carlo simulations. Point-like interactions of photons are modeled using a QPM event generator that incorporates all first-order QED radiative corrections.[14] The QPM events are fragmented via the Lund parton-shower scheme using the default parameters.[†] Diffractively produced hadrons are modeled using the Generalized Vector Meson Dominance model (GVMD).[15] A sample of simulated GVMD events were produced using the techniques developed by the PLUTO group.[16,5] Here a total cross section of $\sigma_{\gamma\gamma}$=240 nb is used and the produced final state is treated as a massive quark-antiquark system that is subsequently converted to hadrons via the Field-Feynman fragmentation scheme.[17] We use the PLUTO-tuned parameters and, like the PLUTO group, limit the p_t distribution by an exp(-5p_t^2) factor.

To simulate resolved photon processes, we have developed the MJET event generator[6] based on the BASES and SPRING programs by Kawabata.[18] MJET generates

[†]In the previous study[6] the LUND string fragmentation scheme was used for the QPM.

events according to the formulae given in ref. 3, using the DG[21] and LAC[22] parametrizations for the parton densities in the photon. According to the results of the simulation, half of the secondary particles from the spectator jets that are characteristic of resolved photon processes can be detected within the angular acceptance of the AMY detector, making these processes distinguishable as events with three or four jets.

The MJET cross section for three- (four-) jet events is given by the product of: the luminosity functions of two photons;[19] the parton density inside one photon (parton densities inside two photons); the subprocess cross section for the interaction between a parton and a photon (between two partons); and a kinematic factor. The subprocess cross sections have been calculated by perturbative-QCD.[20]

Both the DG and LAC parton densities parameterizations are obtained by solving the leading-order Q^2 evolution equation. The Q^2 evolution of the DG parameterization starts from Q_0^2=1 $(GeV/c)^2$ and parameters are fitted to the PLUTO F_2^γ structure function data at Q^2 =5.9 $(GeV/c)^2$ by imposing reasonable relations among the singlet quark, non-singlet quark, and gluon densities.[21] The LAC parameterizations are obtained by fitting parameters to all available F_2^γ experimental data from Q^2 = 1 to 100 $(GeV/c)^2$ without the imposition of any relationships among the parton densities.[22] Three LAC parametrizations are available, LAC1, LAC2 and LAC3, with Q^2 evolutions starting at Q_0^2 = 4.0, 4.0, and 1.0 $(GeV/c)^2$, respectively. We will also compare our data with the GRV parton densities.[23] The GRV densities are obtained from a leading-order QCD evolution with the assumption that the parton density at Q^2 = 0.25 GeV/c^2 is given by GVMD.

In Fig. 1a we compare the photon structure function $F_2^\gamma(x,Q^2) = \sum e_i^2 x q_i(x,Q^2)$ predicted by the DG, LAC, and GRV models, where e_i and q_i are the charge and the quark density of quark flavor i, respectively. Figure 1b shows a comparison of the gluon distributions $xG(x,Q^2)$ predicted by the DG, LAC and the GRV models. The LAC3 model gives an extraordinarily large gluon density at large x. Since the LAC1 and LAC2 are quite similar, we only consider LAC1 here.

As is apparent in Fig. 1, the differences in the quark densities for the DG, LAC, and GRV models are rather small, except for the small x region, $x \leq 0.05$. However, the gluon densities of the three models differ substantially. The QCD scale parameter Q^2 is chosen to be the P_T^2 value of the outgoing partons. In our previous analysis,[6] we treated all quarks as massless and the number of flavors was taken to be four. In the present analysis the mass of the $c-$quark is taken to be 1.6 GeV/c^2 and the number of flavors is taken to be three unless the P_T of the parton exceeds 7 GeV/c for the DG model or, in the case of LAC1, the mass of the $\gamma\gamma$ system exceeds 10 GeV/c^2. The cross section formulae for the subprocesses involving final-state $c-$quarks have been modified to include its mass.

The MJET simulations are carried out by producing two high-P_T partons and one (two) spectator parton(s) corresponding to three- (four-) jet events. Spectator jets are simulated by generating a parton with finite transverse momentum with respect to the incident beam direction, $P_{T,spec}$. Here, the $P_{T,spec}$ distribution is taken to be proportional to $1/(P_{T,spec}^2 + P_{T,spec,0}^2)$ with $P_{T,spec,0}$ = 0.4 GeV/c. The effects of $P_{T,spec}$ values of this order of magnitude on the observed distributions are found to be small.

In order to both guarantee the applicability of QCD and avoid double counting between the soft (diffractive) and hard (non-diffractive) contributions, we only generate events with parton P_T values larger than a cutoff P_T^{min}. Aside from the fact that the applicability of perturbative QCD requires P_T^{min} to be greater than about 1 GeV/c, the appropriate value for the cutoff is not known. Therefore, the value of P_T^{min} is treated as a free parameter and determined from the experimental data as described below. These algorithms are incorporated into the MJET program. The produced partons are hadronized by the Lund string-fragmentation scheme, using the Lund 6.2 program's[24] default values for the fragmentation parameters. Recently, a similar event generator for the resolved processes was implemented in the PYTHIA Monte Carlo generator;[25]

we find that the results from MJET and PYTHIA are similar.

4. The jet-finding algorithm

Jets were found by applying the cone-algorithm that is widely used in hadron-hadron collisions and implemented, for example, in the LUCELL program in JETSET 7.3.[11] The Jade clustering algorithm,[26] which is widely used for e^+e^- annihilation events, was used for comparison and the two algorithms were found to give similar results. In the cone algorithm, all particles within a cone of radius $R = 1$ in psudorapidity η and azimuth ϕ space are combined.[27] The transverse momentum of the jet, P_T^{jet}, is the scalar sum of the transverse momentum within the cones. Initially, the highest p_t particle is used to define the axis of the jet. Subsequently, the jet axis is derived by averaging the individual particle η and ϕ values weighted by their transverse momentum. The resulting jet axis is used to define a new jet cone and this iterative procedure is repeated until the jet cone remains unchanged. Such a jet search is repeated until no further jets are found. Two adjacent jets are combined into one jet if both jet axes are inside the $R = 1$ cone of the combined jet. We only accept jets with two or more particles and with $P_T^{jet} > 2.5$ GeV/c and $|\eta^{jet}| < 1.0$. The $P_T^{jet} > 2.5 GeV/c$ cut minimizes the GVMD contribution and the reduces effects of the choice of P_T^{min}. The $|\eta^{jet}| < 1.0$ cut restricts the jet axes to directions that are well contained in the detector acceptance, where charged (neutral) particles are detected within $|\eta| < 1.5$ (2.2).

We found a total of 1392 jets; 254 events have two jets, and no events have three or more jets. The background contamination for inclusive jets (two-jet events), obtained from Monte Carlo simulations, are;

- hadronic annihilation events: 63.8 ± 5.3 jets (11.5 ± 1.6 events);
- $e^+e^- \rightarrow e^+e^-\tau^+\tau^-$: 56 ± 5.4 jets (8 ± 1.4 events);
- $e^+e^- \rightarrow \tau^+\tau^-$: negligibly small.

The observed jet distributions were corrected by means of a bin-by-bin background subtraction and compared with Monte Carlo simulations. Figure 2(a) shows the inclusive jet transverse momentum distribution. Also shown in the figure are the predictions for GVMD, QPM, and the sum of GVMD, QPM and MJET. Here, in the MJET model we use the LAC1 parton distributions with P_T^{min} values of 2.0, 2.2 and 2.4 GeV/c. As can be seen in the figure, the MJET contribution dominates high transverse momentum jet production in almost-real $\gamma\gamma$ collisions. The GVMD contribution is only significant for P_T^{jet} values below 3 GeV/c. For values of P_T^{jet} below 5 GeV/c, the inclusive jet P_T^{jet}data are well reproduced by the sum of GVMD, QPM and MJET with $P_T^{min} = 2.2$ GeV/c. In Fig. 2(b), the data are compared with the GVMD+QPM+MJET models for the LAC1 and DG parton densities. Here the P_T^{min} value for LAC1 (DG) is set to its optimized value of 2.2 (2.0) GeV/c.[‡] As can be seen in the figure, the DG prediction is similar to that for LAC1 even though the gluon densities for LAC1 and DG are significantly different. We cannot, therefore, discriminate between the LAC1 and DG densities using the P_T^{jet} distribution. Figure 3 shows transverse jet momentum distribution for the inclusive two-jet events. The same conclusions are obtained.

5. Inclusive Jet Cross Sections

In order to obtain an inclusive jet cross section for resolved photon processes, the QPM and GVMD contributions are subtracted from the observed distribution which is then corrected for detector acceptance and resolution (unfolded). The final inclusive cross sections are obtained from the sum of the unfolded cross sections and the QPM cross sections. The unfolding procedure consists of the following series of steps. (Here the $k-th$ bin of the observed distribution for the data is denoted as $N_{data}(k)$.)

- The QPM, GVMD, and the "outside-cut" MJET contributions are subtracted from the data, where the "outside-cut" contribution corresponds to MJET events

[‡]In our previous analysis of the thrust distribution of the AMY 1.0 data[6] we found 1.6 GeV/c as the optimum P_T^{min} value for DG.

with outgoing partons that fail to satisfy either $|\eta| < 1.0$ or $P_t > 2.5\ GeV/c$ but still produce hadron jets that are accepted.

- The acceptance, $\epsilon(i)$, for the $i-th$ bin of the p_t distribution of partons is the ratio of the number of reconstructed jets originated from the $i-th$ bin partons to the number of the $i-th$ bin partons. Here MJET simulations using LAC1 parton densities are used.

- The ratio $frac(i,k)$ is the number of events where the parton's p_t is in the $i-th$ bin and the corresponding reconstructed jet's p_t is in the $k-th$ bin divided by the total number of events in the $k-th$ bin of the reconstructed jet distribution, and is determined using simulated MJET data.

- The $i-th$ bin of the unfolded distribution $N_{gen}(i)$ is then obtained from the expression

$$N_{gen}(i) = \sum_k frac(i,k) N_{data}(k)/\epsilon(i).$$

This unfolding algorithm is correct to the extent that the Monte Carlo simulations accurately describe the observed distributions. Since the observed P_T^{jet} distributions are well reproduced by the GVMD+QPM+LAC1 model, this simple unfolding method is applicable to our data. According to the Monte Carlo simulation, the P_T^{jet} resolution varies from 1 to 2 GeV/c as P_T^{jet} increases from 2.5 to 9 GeV/c.

The resulting inclusive jet and two-jet cross sections for jets with $|\eta| < 1.0$ are shown as a function of P_T in Figs. 4(a) and (b), respectively. The quadratic sum of the statistical and systematic errors are indicated in the figures. The total errors vary from 11% to 29% [13% to 45%] for the inclusive jet [two-jet] events. (Hereafter the bracketed numbers correspond to the results for the two-jet events.) The statistical errors are about 6 to 8% [12 to 25%]. The systematic errors include estimated uncertainties in the luminosity measurements of 1.8%, trigger efficiency of 1.6%, scanning efficiency of

2%, GVMD subtraction (which varies from 10% to 0.5% [3% to 0%] over the range 2.5 $< P_T^{jet} <$ 8 GeV/c) and unfolding procedures (which varies from 26% to 6 % [40% to 5%] over the range 2.5 $< P_T^{jet} <$ 8 GeV/c). The estimated error due to the GVMD subtraction is the variation of the results when the value of $\sigma_{\gamma\gamma}$ is changed by 50%. The systematic error due to the unfolding procedure is the change of the unfolded cross sections when the DG parton density with P_T^{min}= 2.0 GeV/c is used—instead of the LAC1 parton density with P_T^{min}= 2.2 GeV/c—to calculate the correction functions. This difference varies from 26% to 3 % [40% to 1%] over the range 2.5 $< P_T^{jet} <$ 8 GeV/c. The difference in the results when independent fragmentation is used—instead of string fragmentation—gives an additional unfolding error of about 5%.

Since the results correspond to parton-level cross sections, we compare them directly to theoretical calculations in Figs. 4(a) and (b). For resolved process calculations we use the parton densities in the photon given by LAC1, LAC3, DG and GRV models. The data are well described by LAC1, DG and GRV, but the LAC3 parameterization is excluded. Also shown in the figures are the LAC1 predictions with the contributions from the gluon density excluded. The "gluon-off" predictions for DG and GRV are similar to those for LAC1 and not shown in the figures. It is seen that contributions from the gluon density, which amount to nearly half of the cross section, are essential. Even though the gluon densities for these models differ significantly, the jet transverse momentum distributions are almost the same. Thus, the P_T^{jet} distribution is not very sensitive for distinguishing between the LAC1, DG and GRV densities. The TOPAZ group has made a similar analysis using silghtly tighter cut for pseudorapidity of jets, $|\eta^{jet}| < 0.7$ and obtained similar conclusions to ours.[9]

6. Conclusions

We report on measurement of the inclusive jet and two-jet cross sections in almost-real $\gamma\gamma$ collisions at TRISTAN using the AMY detector. The data are in good agreement with leading-order QCD calculations based on either the LAC1, DG, or GRV

parametrizations of the parton densities in the photon. However, the calculation based on LAC3 disagrees with the data.

We thank M. Drees for valuable discussions on resolved photon processes.

References

1. S. Brodsky *et al.*, *Phys. Rev. Lett.* **41** (1978) 672; *Phys. Rev* **D19** (1979) 1418.
2. K. Kajantie and R. Raito, *Nucl. Phys.* **B 159** (1979) 528.
3. M. Drees and R.M. Godbole, *Nucl. Phys.* **B339** (1990) 355.
4. W. Bartel *et al.*(JADE), *Phys. Lett.* **B107** (1981) 163; H. Aihara *et al.*(TPC/2γ), *Phys. Rev.* **D41**; H.-J. Behrend *et al.*(CELLO), *Z. Phys.* **C51** (1991)365.
5. Ch. Berger *et al.*(PLUTO), *Z. Phys.* **C33** (1987) 351.
6. R. Tanaka *et al.*(AMY), *Phys. Lett.* **B277** (1992) 215.
7. T. Ahmed *et al.*(H1), *Phys. Lett.* **B297** (1992) 205.
8. M. Derrick *et al.*(ZEUS), *Phys. Lett.* **B297** (1992) 404.
9. H. Hayashii *et al.*(TOPAZ), KEK-Preprint 93-47, 1993.
10. M. Drees and R. M. Godbole, *Phys. Rev. Lett.* **67** (1991) 1189; P. Chen, *Proc. of the IXth Int. Workshop on Photon-Photon Collisions*, San Diego, California (1992) p418; M Drees, *ibid*, p430; J.R. Forshaw and J.K. Storrow, *ibid*, p442.
11. T. Sjöstrand, *CERN-TH-6488-92* (May 1992) 284p.
12. T. Sjöstrand, and H. Bengtsson *Comp. Phys. Comm* **43** (1987) 367.
13. T. Kumita *et al.*(AMY), *Phys.Rev.* **D42** (1990) 1339.
14. M. Kuroda, *Meiji Gakuin Univ. (Tokyo) Research J.***424** (1988) 27.
15. J.J. Sakurai and D. Schildknecht, *Phys. Lett.* **B40** (1972) 121.
16. Ch. Berger *et al.*(PLUTO), *Z. Phys.* **C26** (1984) 191;29 (1985)499.
17. R.D. Field and R.P. Feynman, *Nucl. Phys.* **B136** (1978) 1.
18. S. Kawabata, *Comp. Phys. Comm* **41** (1986) 127.
19. To take into account the anti-tag condition we used the luminosity function given in eq.(2.19) of Ch. Berger and W. Wagner, *Phys. Rep.* **146** (1987) 1.

20. D.W. Duke and J.F. Owens, *Phys. Rev.* **D26** (1982) 1600; B.L. Combridge *et al.*, *Phys. Lett.* **B70** (1977) 234; M. Gluck *et al.*, *Phys. Rev* **D18** (1978) 1501.
21. M. Drees and K. Grassie, *Z. Phys.* **C28** (1985) 451.
22. A. Levy, H. Abramowics, and K. Charchula, *Phys. Lett.* **B269** (1991) 458.
23. M. Gluck, E. Reya and A. Vogt, *Phys. Rev.* **D46** (1992) 1973.
24. T. Sjöstrand *Comp. Phys. Comm* **39** (1986) 347.
25. T. Sjöstrand, *CERN-TH-6488-92* (May 1992) p284.
26. W. Bartel *et al.*(JADE), *Z. Phys.* **C33** (1986) 23.
27. S.D. Ellis *et al.*, *Phys. Rev.* **D40**(1989) 2188.

Figure Captions

Fig. 1.a) A comparison of the photon structure function $F_2^\gamma(x, Q^2)$ at Q^2 = 10 (GeV/c)^2, calculated using the LAC1, LAC2, LAC3, DG and GRV parton densities. b) A similar comparison of the gluon distribution $xG(x, Q^2)$ in the photon at Q^2 = 10 (GeV/c)^2. The solid, dot-dash, dashed, dotted and double-dot-dash curves represent the LAC1, LAC2, LAC3, DG and GRV predictions, respectively. The number of flavor is assumed to be three.

Fig. 2. Comparisons of the observed transverse momentum of jets with Monte Carlo simulations. a) The histograms are the predictions of i) GVMD (lower dotted), ii) QPM (dash-dot), and iii) QPM + GVMD + MJET where MJET is simulated for the LAC1 parton densities with P_T^{min} =2.0 GeV/c (dashed), P_T^{min} =2.2 GeV/c(solid) and P_T^{min} =2.4 GeV/c (upper dotted). b) The histograms are the QPM + GVMD + MJET expectation where MJET is simulated for the LAC1 parton densities with P_T^{min} =2.2 GeV/c (solid), and the DG parton densities with P_T^{min} =2.0 GeV/c (dashed). Only statistical errors are shown.

Fig. 3. The same as Fig.2 for the inclusive two-jet events.

Fig. 4. Inclusive jet a) and two-jet b) cross sections as a function of P_T^{jet} integrated over $|\eta| < 1.0$. The curves represent the sum of the QPM (direct) and MJET (resolved) cross sections using the LAC1 (solid), GRV (dash double-dot), DG (dotted), LAC3 (dashed), and LAC1 with the gluon components excluded (dash dotted) parton densities. The short-dashed curve represents the QPM cross section. The plotted errors are the quadrature sum of the statistical and systematic errors.

Fig. 1

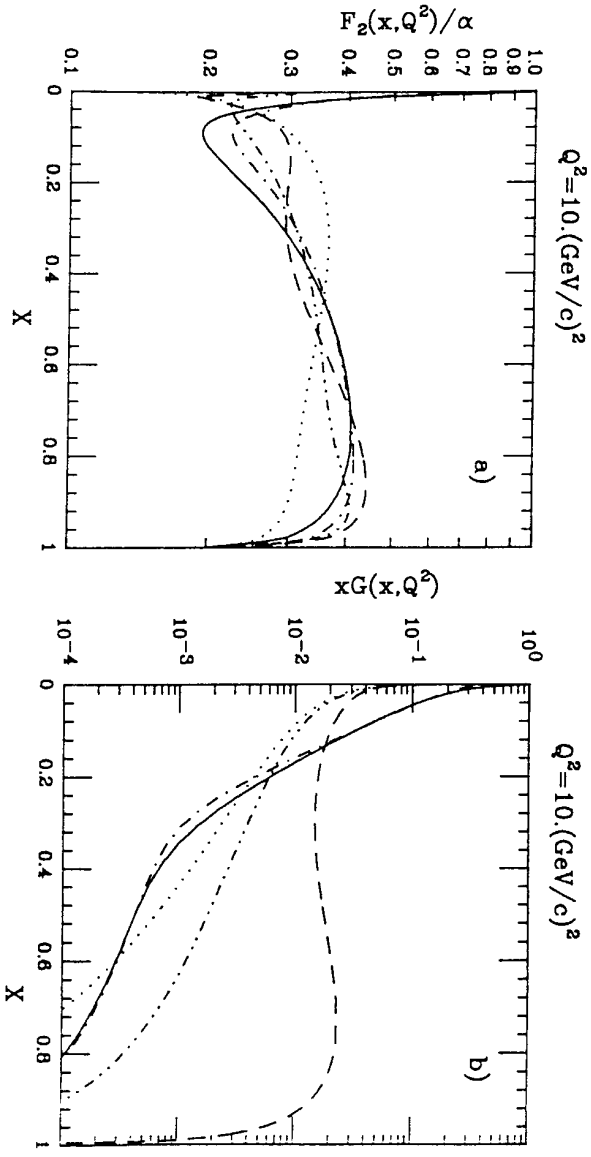

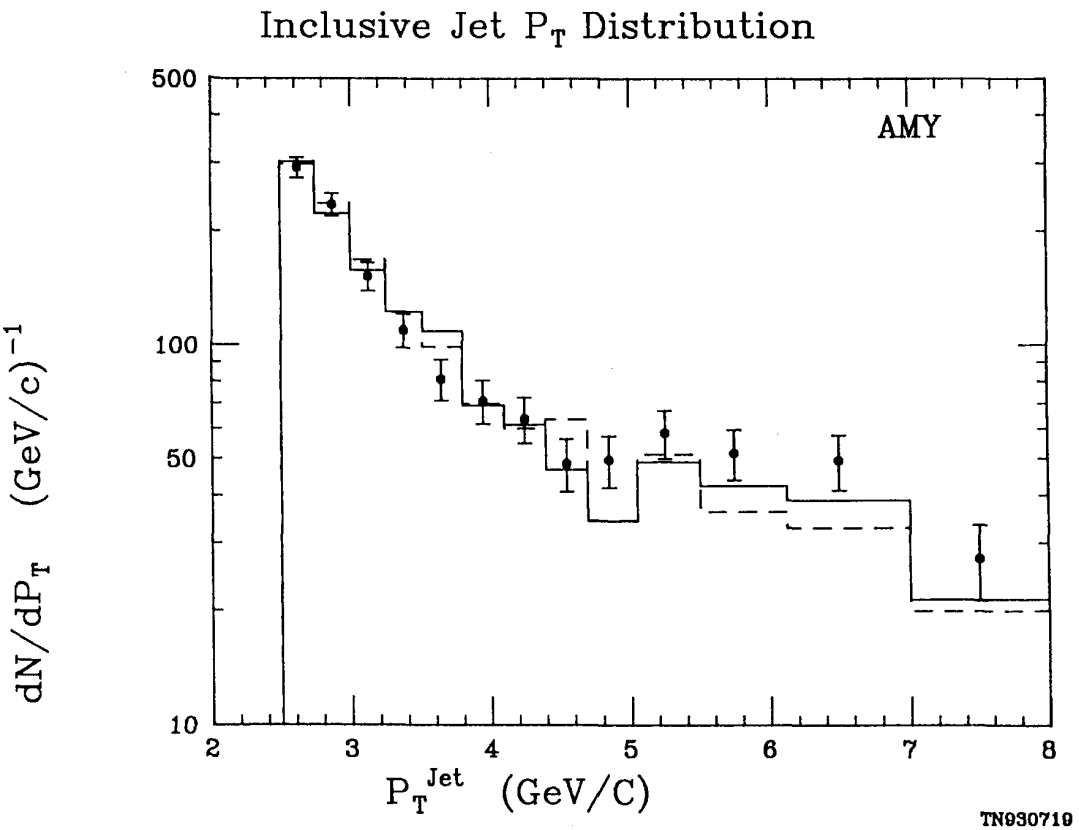
Inclusive Jet P_T Distribution
AMY
500
100
50
10
2
3
4
5
6
7
8
dN/dP_T $(GeV/c)^{-1}$
P_T^{Jet} (GeV/C)
TN930719

Fig. 2(b)

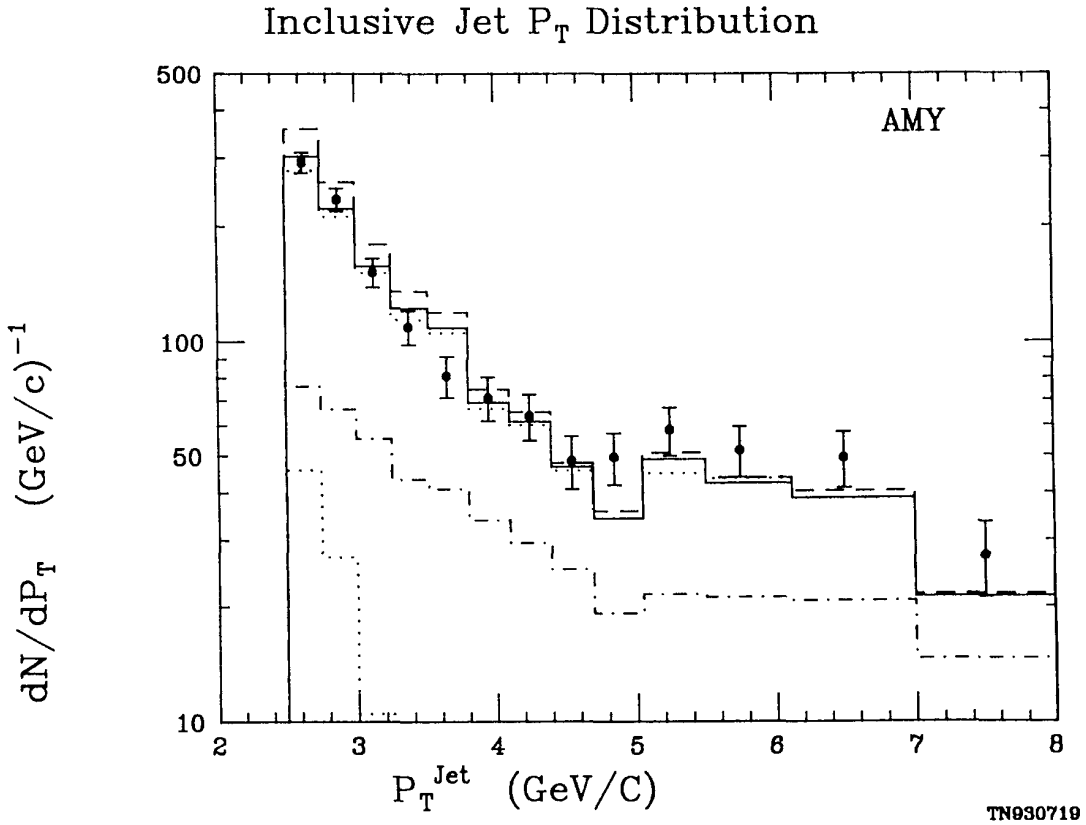
Inclusive Jet P_T Distribution
AMY
500
100
50
10
2
3
4
5
6
7
8
dN/dP_T $(GeV/c)^{-1}$
P_T^{Jet} (GeV/C)
TN930719

Fig. 2(a)

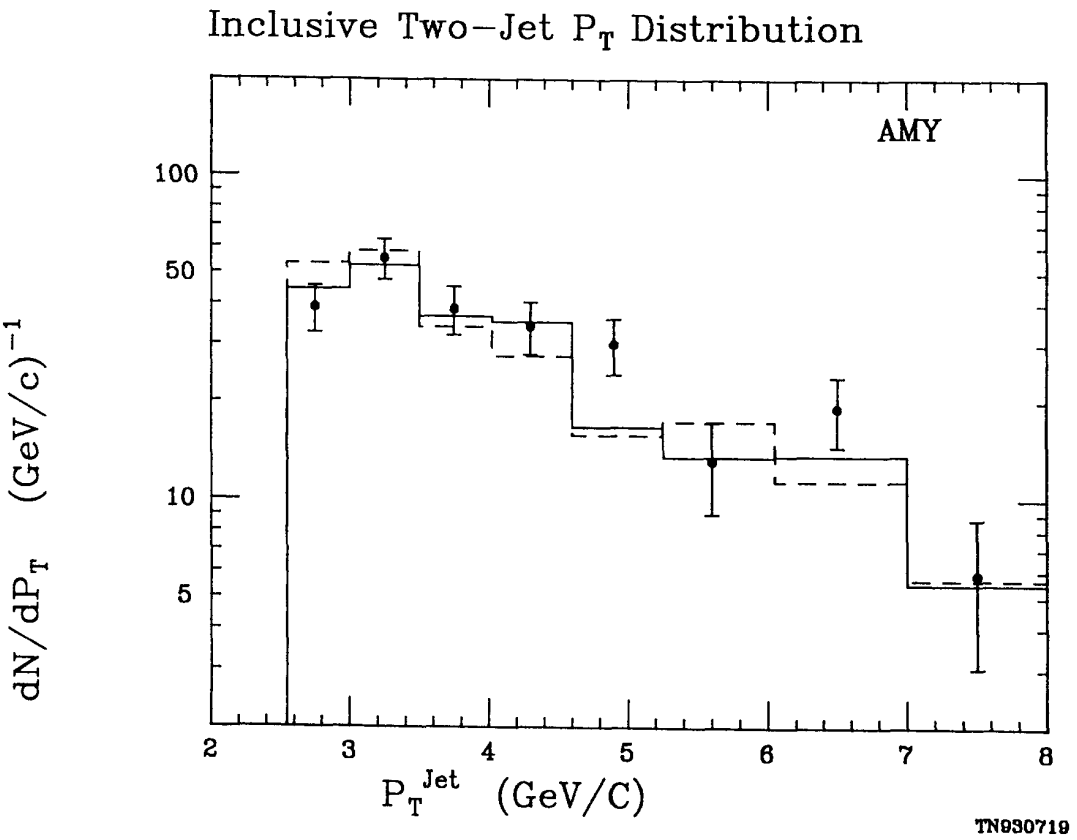
Inclusive Two−Jet P_T Distribution
AMY
100
50
10
5
2
3
4
5
6
7
8
dN/dP_T $(GeV/c)^{-1}$
P_T^{Jet} (GeV/C)
TN930719

Fig. 3(b)

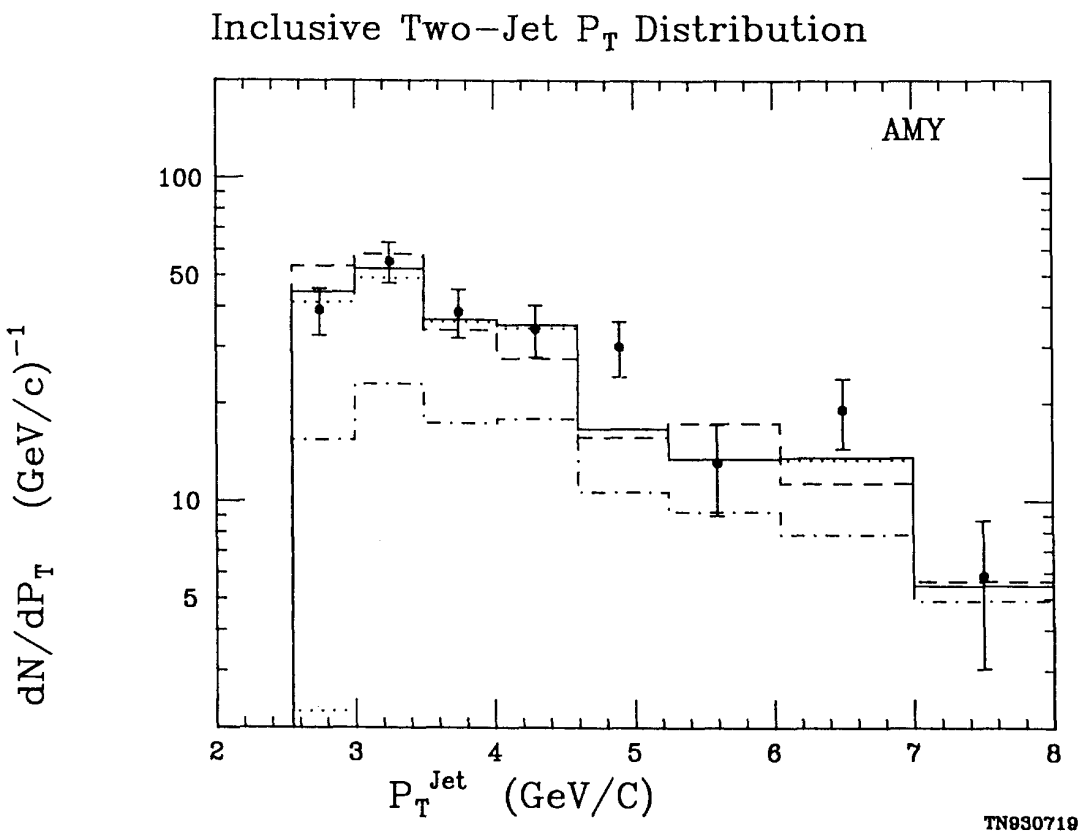
Inclusive Two−Jet P_T Distribution
AMY
100
50
10
5
2
3
4
5
6
7
8
dN/dP_T $(GeV/c)^{-1}$
P_T^{Jet} (GeV/C)
TN930719

Fig. 3(a)

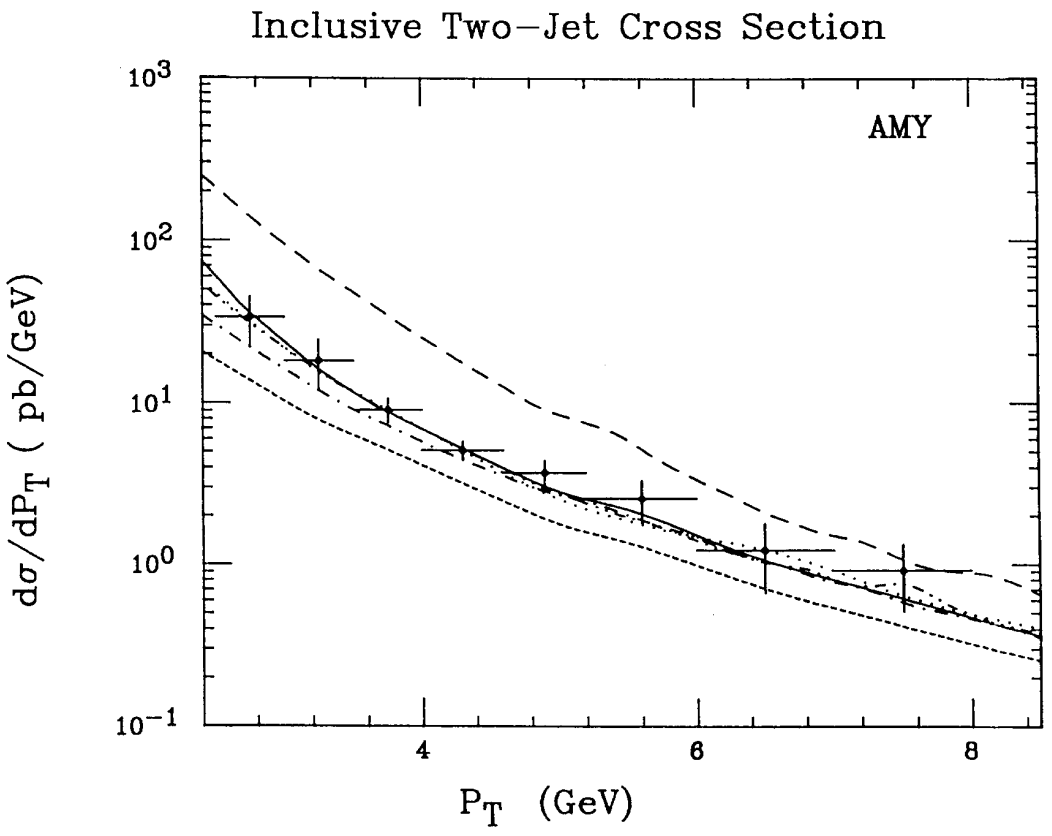
Inclusive Two−Jet Cross Section
AMY
10^3
10^2
10^1
10^0
10^{-1}
4
6
8
$d\sigma/dP_T$ (pb/GeV)
P_T (GeV)

Fig. 4(b)

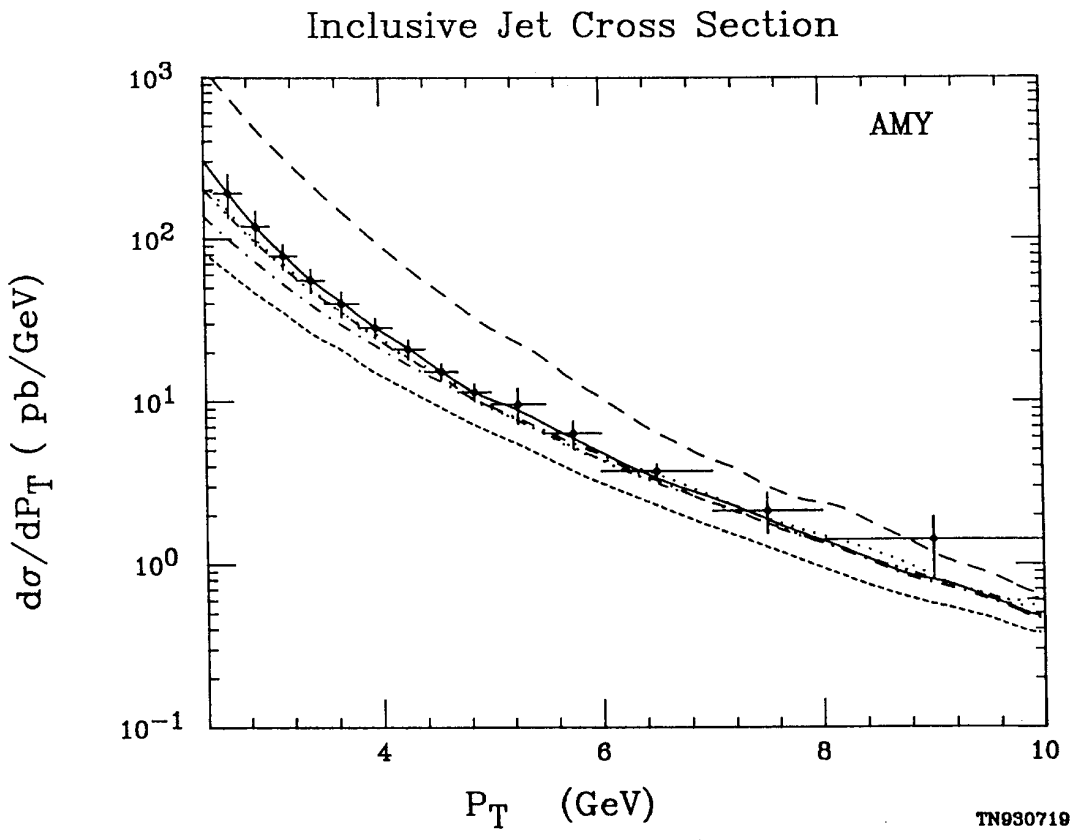
Inclusive Jet Cross Section
AMY
10^3
10^2
10^1
10^0
10^{-1}
4
6
8
10
$d\sigma/dP_T$ (pb/GeV)
P_T (GeV)
TN930719

Fig. 4(a)